Fatigue Properties of Cold-Rolled Cu-Zr Alloy Sheets

R. Niu, K. Han, V. J. Toplosky, and J. Toth

Abstract—**We performed tension-tension fatigue tests in stress control mode on cold-rolled Cu-Zr alloy sheets with various levels of tensile strength (TS). We then compared the fatigue properties of these sheets to those of cold-rolled Cu sheets. Fatigue life increased as TS increased. We separated our Cu-Zr sheets according to their mechanical strength levels, designating those with their TS ∼490 MPa as "H", those with TS around 448 ± 5 MPa as "M", and those with TS < 440 MPa as "L". The "H" sheets exhibited the longest life, followed by the "M" sheets, and the "L" sheets, all outperforming Cu. At 390 MPa. "H" Cu-Zr's fatigue life was ∼3 times that of Cu. Both the Cu-Zr and the Cu showed cyclic hardening. The presence of Zirconium improved fatigue life by stabilizing microstructure and retarding the formation of cracks during fatigue cycling, thus positioning Cu-Zr alloys as much stronger candidates than Cu for resistive magnet conductors.**

Index Terms—**Fatigue, Cu-Zr, fatigue life, cyclic hardening, particle, cold-roll.**

I. Introduction

Cu-BASED composites are widely used in applications requiring high mechanical strength and electrical conductivity, such as conductor sheets in resistive magnets. Strength is typically enhanced through cold working [1], [2], grain refinement [3], [4], and nano-particles dispersion strengthening [5], [6], [7], [8], [9]. Typical conductor sheets for resistive magnet are heavily deformed Cu-based metal-metal composites, such as Cu-Zr [2], [9], [10], Cu-Ag [11], [12], [13], [14], and Cu [15], [16].

In addition to high-tensile strength and high electric conductivity, life is a critical issue that needs to be addressed, because a solid knowledge of cyclic deformation response, fatigue life, and cyclic stability of these materials is crucial for the lifetime of magnets.

Previous studies on Cu reveal diverse fatigue behaviors: single crystals and annealed polycrystalline Cu exhibit cyclic hardening under low-cycle fatigue [17], while heavily cold-drawn (99% reduction in area) or severely plastically deformed (SPD) Cu shows cyclic softening [18], [19], [20], [21]. Specifically, higher plastic strain amplitudes promote cyclic softening and grain coarsening [21].

Received 25 July 2025; revised 3 October 2025; accepted 26 October 2025. Date of publication 24 November 2025; date of current version 9 December 2025. The work was supported in part by the National Science Foundation under Grant DMR-1157490 and Grant DMR-1644779, and in part by the State of Florida. *(Corresponding author: Ke Han.)*

The authors are with the National High Magnetic Field Laboratory, Tallahassee, FL 32309 USA (e-mail: han@magnet.fsu.edu).

Color versions of one or more figures in this article are available at https://doi.org/10.1109/TASC.2025.3636496.

Digital Object Identifier 10.1109/TASC.2025.3636496

Cyclic softening is linked to the cooperative mechanisms of dislocation recovery, dynamic recrystallization, and grain coarsening [22], [23], [24], [25]. Adding Zr to Cu stabilizes the microstructure in SPD-processed alloys [9], enhancing cyclic stability of Cu by exhibiting longer fatigue lives and notable cyclic hardening [2], [26].

While SPD-processed Cu and Cu alloys have been extensively studied [22], [27], [28], [29], [30], [31], [32], the fatigue behavior of heavily cold-rolled Cu-Zr sheets—key for resistive magnet applications—remains underexplored, especially under stress-controlled conditions mimicking operational hoop stresses. This study investigates the fatigue properties of cold-rolled Cu-Zr sheets with varying TS and compares them to cold-rolled Cu, aiming to establish fatigue life relationships and cyclic deformation behavior under stress control.

II. Experimental Methods

A. Materials and Fabrication

Cold-rolled copper alloy C15100 (Copper Zirconium) with different strength levels were manufactured by Wieland Metals. Cold-rolled Cu (UNS C10700) sheets with similar strength were chosen to compare the fatigue properties. The nominal thickness was 0.77 mm for Cu-Zr and 0.75 mm for Cu.

B. Mechanical Tests

Tensile specimens were made following ASTM E8M standards, with a gauge length of 50 mm and width of 8.78 mm in a dog-bone shape. Longitudinal direction (Ld) samples were aligned parallel to the rolling direction (Rd), and transverse direction (Td) samples were perpendicular to Rd. Tensile tests were conducted on a servo-hydraulic MTS machine with a 10 KN load cell and a 25 mm clip-on extensometer.

Cu-Zr sheets were classified by Ld tensile strength levels: "H" (∼490 MPa), "M" (448 ± 5 MPa), and "L" (<440 MPa). Due to lower strength in longitudinal direction (see Table I), fatigue tests were focused on this direction. Tension-tension fatigue tests (stress ratio $R = 0.1$) were performed under normal stress control at 1 Hz on the same MTS machine. Maximum stresses (σ_max) were 479, 445, 434, 410, 400 and 390 MPa. 390 MPa was the design strength for perfect CuZr sheets (TS ∼ 490 MPa) for magnets.

C. Microstructure Preparation

Microstructure was investigated in a FEI Helios G4 UC Field Emission Scanning Electron Microscope (FESEM). For

TABLE I
0.77 MM THICK CUZR TENSILE RESULTS

Samples	YS, MPa	TS, MPa	Elongation, %	RA %	TS/YS	Conductivity %,IACS
Longitudinal direction						
H						
H	478	489	6.6	72	1.02	91.2
M						
M1	436	454	7.8	81	1.04	91.6
M2	431	448	7.8	77	1.04	90.0
M3	432	445	7.7		1.03	90.1
M4	434	445	5.7		1.03	93.3
L						
L1	418	432	4.0		1.03	94.3
L2	416	432	4.2		1.04	95.2
L3	411	428	4.0	83	1.04	95.4
Cu						
Cu	421	440	8.3	86	1.05	96.1
Transversal direction						
H	479	494	4.6		1.03	90.6
L1	442	457	4.9		1.03	94.2
Cu	459	465	3.7		1.01	96.3

YS, TS, and RA represent the yield strength, tensile strength, and reduction-in-area, respectively.

chemistry examinations, an Energy Dispersion X-ray (EDX) spectrometer was used.

III. RESULTS AND DISCUSSIONS

A. Mechanical Test Results

Our "H", "M", and "L" Cu-Zr samples exhibited different tensile strength (see Table I). We found that the electrical conductivity of the "L" Cu-Zr was the highest of the three categories. This finding reflects a typical trade-off between strength and conductivity. The strength of our Cu sheets (as opposed to CuZr) was between that of "M" and "L." The electrical conductivity of Cu, however, was higher than that of any Cu-Zr. The ratio of tensile strength to yield strength (TS/YS), measured in the longitudinal direction, was estimated to be 1.02 in "H" and 1.03∼1.04 in "M" and "L." The ratio difference between "H", "M," and "L" was so small that their work-hardening capacity was considered identical. Similar low values were also found in high-strength Cu-Ag [33]. Such low ratios suggest a defect-saturated microstructure with limited work-hardening capacity [13]. Like cold-rolled Cu-Zr, cold-rolled Cu exhibited a TS/YS ratio of 1.05 along the Ld, despite the different strengthening mechanisms.

We performed independent t-test to assess whether there is a significant difference in the TS/YS ratio across the "H," "M," and "L". The p-value for the ratio was calculated as 1.2×10^{-6} between "H" and "M," and 0.23 between "M" and "L." Conventionally, a p-value below 0.05 ($p < 0.05$) is deemed statistically significant. This suggests that the difference observed between "H" and "M" is likely statistically significant.

In addition to low work-hardening rates in our Cu-Zr cold-rolled samples, we also observed pronounced strain localization, which was accompanied by local extrusions or intrusions (i.e., found within 400 μm of fracture surfaces, see Fig. 1(a)). We assumed that the local extrusions and intrusions that we observed in our Cu-Zr samples could have resulted from the presence of Zr in the sample. On the other hand, our cold-rolled Cu samples exhibited numerous extrusions and intrusions that were non-local– i.e., that were distributed across the entire gauge length of the fatigue samples (Fig. 1(b)). The spreading of extrusions and intrusions in cold-rolled Cu indicated a high degree of homogeneous deformation. This is consistent with our observation in Cu of both high elongation and high reduction-in-area (RA).

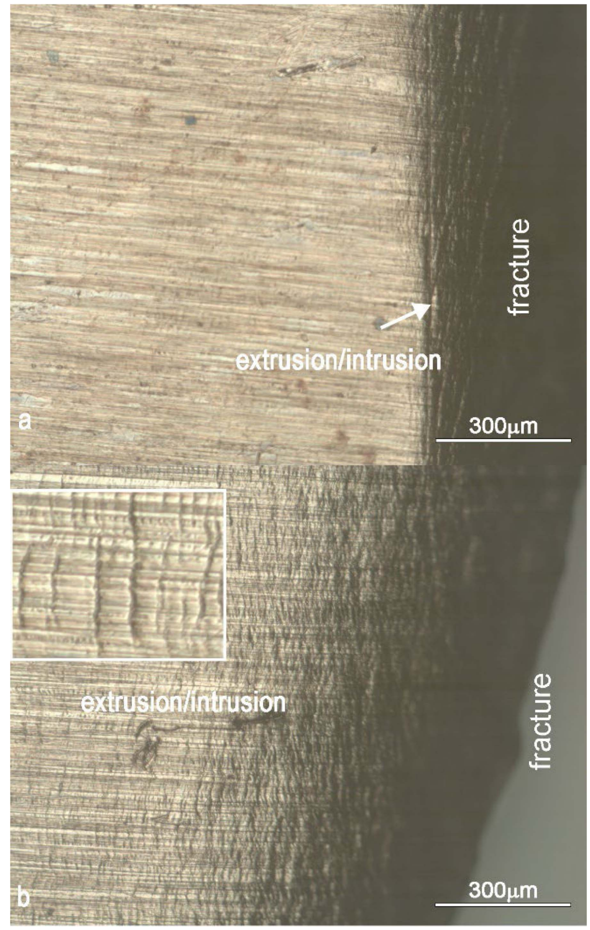

Fig. 1. Surface extrusions/intrusion on fractured fatigue samples tested at maximum fatigue stress of 390MPa. (a) The extrusions and intrusions sitting at fracture regions in the "H" Cu-Zr. (b) The extrusions/ intrusions extend across the gauge length of Cu sample. The inset shows magnified ones. Long and dense ones distribute near fracture. The distribution became sparse and short with the distance to fracture increase.

B. Fatigue Life

Under equivalent fatigue stress levels, Cu-Zr samples with higher TS displayed longer fatigue life than similar samples with lower TS. At all stress levels, the "H" samples had the longest fatigue life. The fatigue life of the "M" samples fell between that of the "H" and the "L." Fig. 2 shows that the number of cycles-to-failure (i.e., fatigue life, N) was dependent on maximum stress ($\sigma_{\max}$). The "H" samples sustained about 8000 cycles at their

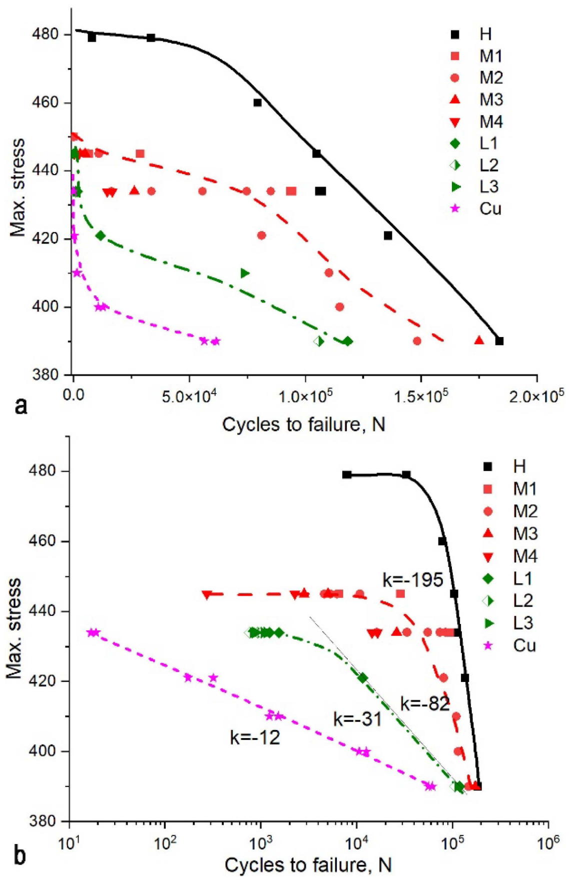

Fig. 2. The dependence of N on the maximum.stress at the stress ratio R = 0.1. (a) x-axis in normal form. (b) x-axis in logarithmic form.

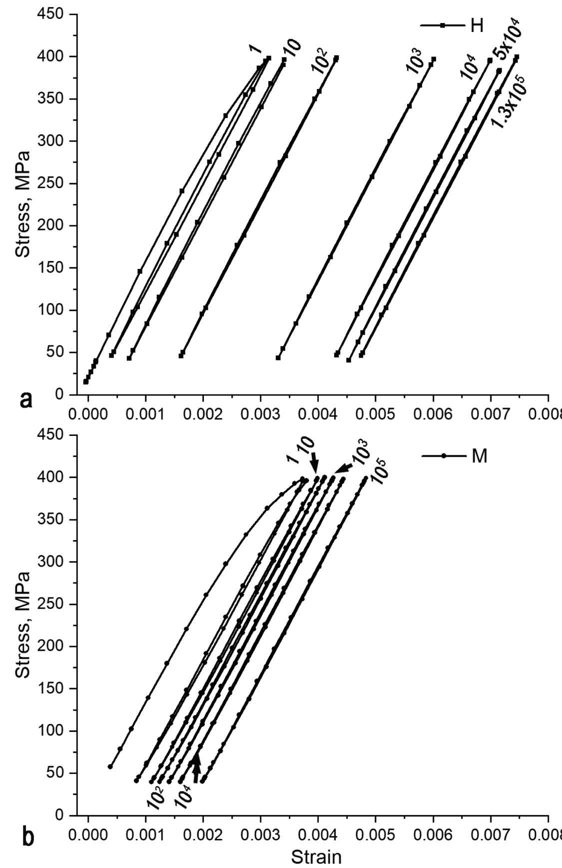

Fig. 3. Stress–strain hysteresis loops at different cycles under 400 MPa maximum stress level. (a) Data from a "H" sample. (b) Data from a "M" sample.

yield strength (479 MPa.) At a fatigue stress of 434 MPa (i.e., the yield strength of the "M" samples), the N of the "H" samples was ~105k, almost 6 times as long as the N (~18k) of M1. The value of N increased significantly as long as the $\sigma_{\max}$ remained below the yield strength. The "H" samples endured ~106k cycles at 434 MPa and ~184k cycles at 390 MPa. The respective values of N for the "M" and the "L" samples increased to ~162k cycles and ~112k cycles at 390 MPa. Both the "M" and the "L" samples had shorter fatigue lives than the "H".

Small variations in TS produced large differences in N. The TS of M1 was 6 MPa higher than that of M2. At 445 MPa, however, the average N of M1 was about two times higher than that of M2. Similarly, a difference of 9 MPa between M1 and M4 led to a 93% reduction in the average N of M4.

Although the strength of the "L" samples was about 10 MPa lower than that of Cu samples, the "L" still endured more cycles than Cu, which sustained 59k cycles at 390 MPa, about half the fatigue life of the "L" (see Fig. 2(a)).

The declining part of the S–N curve begins at a total number of cycles of 10^4 for the "H," 10^4 for the "M," 10^3 for the "L," and 10 for Cu. The slope of the declining part of $\sigma_{\max}$ vs. log (N) depends on the strength of the materials involved. The average slope, k, values for the "H," the "M," the "L," and Cu were measured as −195, −82, −31, and −12, respectively (see Fig. 2(b)).

C. Cyclic Stress-Strain Curves

The stress-strain hysteresis loops obtained from both the Cu and Cu-Zr alloys showed difference in their cyclic deformation behaviors (Figs. 3 and 4). Relatively larger plastic deformation occurred mainly in materials below ten cycles.

For example, under 400 MPa maximum stress level, a comparison of hysteresis loops at cycles 1, 10, 10^2, 10^3, 10^4, 5×10^4, and 1.3×10^5 indicated that, for "H" Cu-Zr samples, the 1st cycle displayed the largest plastic deformation strain. After 10 cycles, the energy dissipated per cycle (i.e., the area enclosed by the loop) became smaller. At 100 cycles, the material reached a stable state, where its hysteresis loops were almost linear and energy dissipation was very small. The plastic strain range measured from the loops was 9.1×10^{-5} in the 1st cycle, 5.6×10^{-5} in the 10th cycle, 3.7×10^{-5} in the 100th cycle, 2.9×10^{-5} in 10^3th cycle, 2.8×10^{-5} in 10^4th cycle, 2.7×10^{-5} in 5×10^4th cycle, and 2.5×10^{-5} in 1.3×10^5th cycle (see Fig. 5). The plastic strain range reducing with fatigue cycles suggested cyclic hardening.

A comparison of hysteresis loops at cycles 1, 10, 10^2, 10^3, 10^4, and 10^5 indicated that the "M" Cu-Zr behaved similar to "H". The 1st cycle displayed large plastic deformation strain, and after 10 cycles, the energy dissipated per cycle became smaller. Overall, the energy dissipation was smaller in the "M" than in the "H". The plastic strain range was 3.9×10^{-5} at the 100th

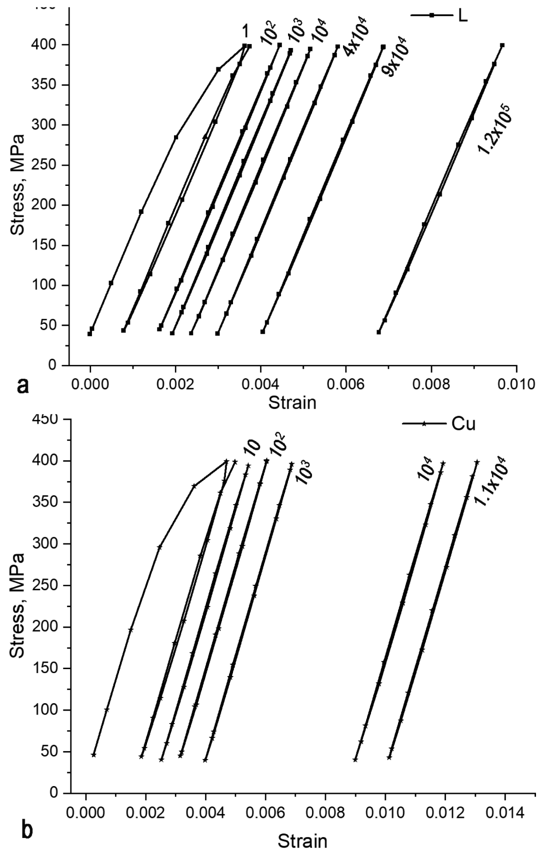

Fig. 4. Stress-strain curves of (a) "L" Cu-Zr, and (b) Cu.

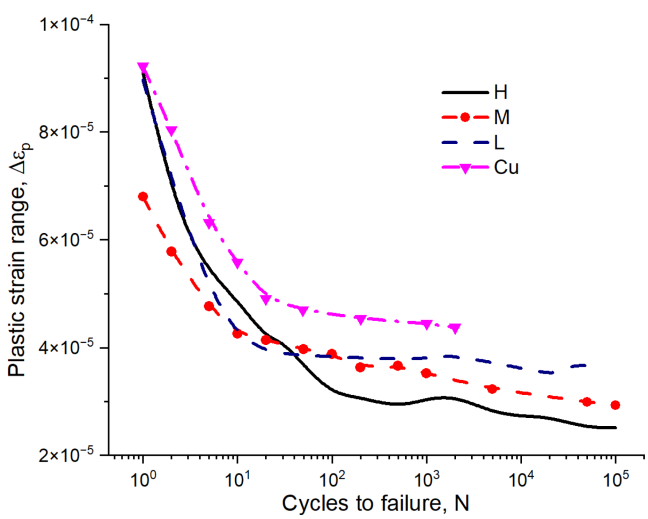

Fig. 5. Fatigue life as a function of plastic strain range for "H", "M", and "L" Cu-Zr and Cu.

cycle, and reduced to 3.5×10^{-5} in the 10^3th cycle and 3.0×10^{-5} in the 10^4th cycle and 2.9×10^{-5} in the 10^5th cycle. As the "H", the cyclic hardening was discovered as well.

In both the "L" Cu-Zr and Cu samples, the hysteresis loops evolution with cycles were similar to those of the "H" and "M" ones. After 10 cycles, the energy dissipated per cycle became smaller. In the "L", the plastic strain range was 4.3×10^{-5} in the 10th cycle, and decrease to 3.8×10^{-5} in the 10^3th cycle

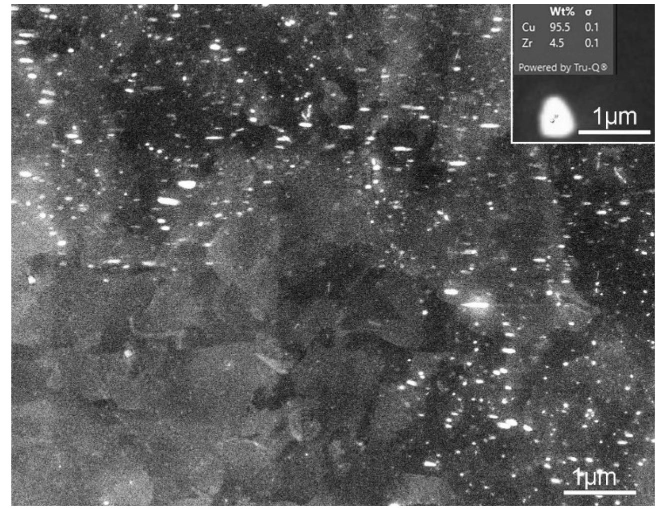

Fig. 6. SEM images showing the microstructure of a sample from "L" Cu-Zr. White particles are rich in Zr. An inset shows an SEM image with EDS result of a 500 nm sized particle. In particle rich region, the average particle size is about 54 nm. The average particle spacing is approximately 260 nm.

and 3.6×10^{-5} in the 10^4th cycle. In the Cu, the plastic strain range was 5.6×10^{-5} in the 10th cycle, and decreased to 4.5×10^{-5} in the 10^3th cycle. Cyclic hardening occurred but appeared smaller than the "H" in cycles greater than 100.

Comparing with the "H" and "M" and "L", the Cu showed the highest plastic strain range in the stable stage under 400 MPa maximum fatigue stress, and the "H" showed the lowest plastic strain range. The plastic strain range in the stable stage appeared to be inversely proportional to the strength of materials. The "M" and "L" had a similar value at this fatigue stress level.

Meanwhile, the stress-strain hysteresis loops shifted progressively along the strain axis. Because of the tension-tension loading, there was a net plastic strain after each cycle. The directional accumulation of plastic strain led to plastic ratcheting. Plastic ratcheting was demonstrated in each material.

D. Microstructure

The plan-view microstructure of the "L" Cu-Zr sheets indicated the non-uniformity distribution of particles. Some regions were covered by high-density of particles embedded in the matrix, while others had none, see Fig. 6. This might be one of the reasons for the relative low strength and fatigue life in the "M" and "L" Cu-Zr. More work is underway to explore the microstructure difference among these different stress-leveled Cu-Zr alloys.

In particle rich regions, a multi-modal particle distribution within the Cu matrix was depicted. Most of the particles appeared as round white features, with a smaller proportion exhibiting short rod-like shapes. The round particles measured approximately tens of nanometers in diameter, while the short rods ranged from 200 to 700 nm in length. These small particles uniformly distributed within grain interiors, and no evident segregation at grain boundaries was observed SEM-EDS results indicated higher Zr concentrations in white particles than in the matrix. In other words, these white particles were Zr-rich. In a 500 nm-sized particle, the Zr concentration was detected to be 4.5 wt%, see the inset in Fig. 6.

IV. Conclusion

In stress-controlled, tension-tension fatigue tests, cold-rolled Cu-Zr sheets had longer fatigue life than cold-rolled Cu sheets. For Cu-Zr sheet themselves, the higher the tensile strength, the longer the fatigue life and the lower plastic strain range. Cyclic hardening was revealed in both Cu-Zr and Cu sheets.

Acknowledgment

The authors would like to thank Mary Tyler for editing.

References

[1] J. D. Verhoeven et al., "Development of deformation processed copper-refractory metal composite alloys," *J. Mater. Eng.*, vol. 12, no. 2, pp. 127–139, Jun. 1990, doi: 10.1007/BF02834066.

[2] H. Kimura, A. Inoue, N. Muramatsu, K. Shin, and T. Yamamoto, "Ultrahigh strength and high electrical conductivity characteristics of Cu-Zr alloy wires with nanoscale duplex fibrous structure," *Mater. Trans.*, vol. 47, no. 6, pp. 1595–1598, 2006, doi: 10.2320/matertrans.47.1595.

[3] K. Han, R. P. Walsh, A. Ishmaku, V. Toplosky, L. Brandao, and J. D. Embury, "High strength and high electrical conductivity bulk Cu," *Philos. Mag.*, vol. 84, no. 34, pp. 3705–3716, Dec. 2004, doi: 10.1080/14786430412331293496.

[4] R. Niu and K. Han, "Strain hardening and softening in nanotwinned Cu," *Scripta Materialia*, vol. 68, no. 12, pp. 960–963, Jun. 2013, doi: 10.1016/j.scriptamat.2013.02.051.

[5] A. Morozova, R. Mishnev, A. Belyakov, and R. Kaibyshev, "Microstructure and properties of fine grained Cu-Cr-Zr alloys after termo-mechanical treatments," *Rev. Adv. Mater. Sci.*, vol. 54, no. 1, pp. 56–92, 2018, doi: 10.1515/rams-2018-0020.

[6] B. An, Y. Xin, R. Niu, J. Lu, E. Wang, and K. Han, "Hardening Cu-Ag composite by doping with Sc," *Mater. Lett.*, vol. 252, pp. 207–210, 2019.

[7] K. Han, R. E. Goddard, V. Toplosky, R. Niu, J. Lu, and R. Walsh, "Alumina particle reinforced Cu matrix conductors," *IEEE Trans. Appl. Supercond.*, vol. 28, no. 3, Apr. 2018, Art. no. 7000305, doi: 10.1109/TASC.2018.2795587.

[8] R. Niu, V. J. Toplosky, J. W. Levitan, J. Lu, and K. Han, "Deformation induced precipitation in CuCrZr composites," *Mater. Sci. Eng., A*, vol. 875, Jun. 2023, Art. no. 145092, doi: 10.1016/j.msea.2023.145092.

[9] R. P. Singh, A. Lawley, S. Friedman, and Y. V. Murty, "Microstructure and properties of spray cast Cu Zr alloys," *Mater. Sci. Eng., A*, vol. 145, no. 2, pp. 243–255, Oct. 1991, doi: 10.1016/0921-5093(91)90254-K.

[10] M. D. Bird, S. Bole, Y. M. Eyssa, B. J. Gao, and H. J. Schneider-Muntau, "Test results and potential for upgrade of the 45 T hybrid insert," *IEEE Trans. Appl. Supercond.*, vol. 10, no. 1, pp. 439–442, Mar. 2000, doi: 10.1109/77.828266.

[11] S. Tardieu et al., "Influence of bimodal copper grain size distribution on electrical resistivity and tensile strength of silver - copper composite wires," *Mater. Today Commun.*, vol. 37, Dec. 2023, Art. no. 107403, doi: 10.1016/j.mtcomm.2023.107403.

[12] S. Tardieu et al., "High-strength copper/silver alloys processed by cold spraying for DC and pulsed high magnetic fields," *Magnetochem.*, vol. 10, no. 3, 2024, Art. no. 15. [Online]. Available: https://www.mdpi.com/2312-7481/10/3/15

[13] R. Niu and K. Han, "Pockets of strain-softening and strain-hardening in high-strength Cu-24wt%Ag sheets," *J. Mater. Sci.*, vol. 58, no. 21, pp. 8981–8989, Jun. 2023, doi: 10.1007/s10853-023-08519-y.

[14] C. A. Davy, K. Han, P. N. Kalu, and S. T. Bole, "Examinations of Cu-Ag composite conductors in sheet forms," *IEEE Trans. Appl. Supercond.*, vol. 18, no. 2, pp. 560–563, Jun. 2008, doi: 10.1109/TASC.2008.922510.

[15] D. B. Mark, "Resistive magnet technology for hybrid inserts," *Supercond. Sci. Technol.*, vol. 17, no. 8, Jun. 2004, Art. no. R19, doi: 10.1088/0953-2048/17/8/R01.

[16] J. Toth and S. Bole, "Conceptual design for a next generation resistive large bore magnet at the NHMFL," *IEEE Trans. Appl. Supercond.*, vol. 30, no. 4, Jun. 2020, Art. no. 4300104, doi: 10.1109/TASC.2020.2964219.

[17] C. E. Feltner and C. Laird, "Cyclic stress-strain response of F.C.C. metals and alloys—II dislocation structures and mechanisms," *Acta Metallurgica*, vol. 15, pp. 1633–1653, 1967.

[18] E. Jiménez-Ruiz, R. Lostado-Lorza, and C. Berlanga-Labari, "A comprehensive review of fatigue strength in pure copper metals (DHP, OF, ETP)," *Metals*, vol. 14, no. 4, 2024, Art. no. 464, [Online]. Available: https://www.mdpi.com/2075-4701/14/4/464

[19] H. Zhi and H. Zhao, "Low cycle fatigue behavior of Cu-Cr-Zr-La alloys," *J. Phys., Conf. Ser.*, vol. 2951, no. 1, Feb. 2025, Art. no. 012133, doi: 10.1088/1742-6596/2951/1/012133.

[20] W. A. Spitzig, L. K. Reed, and A. Chatterjee, "Comparison of the low-cycle fatigue properties of heavily cold-drawn copper and Cu-20%Nb," *Mater. Sci. Eng., A*, vol. 123, no. 1, pp. 69–74, Jan. 1990, doi: 10.1016/0921-5093(90)90211-K.

[21] H. W. Höppel, Z. M. Zhou, H. Mughrabi, and R. Z. Valiev, "Microstructural study of the parameters governing coarsening and cyclic softening in fatigued ultrafine-grained copper," *Philos. Mag. A*, vol. 82, no. 9, pp. 1781–1794, Jun. 2002, doi: 10.1080/01418610208235689.

[22] Z. S. Basinski and S. J. Basinski, "Fundamental aspects of low amplitude cyclic deformation in face-centred cubic crystals," *Prog. Mater. Sci.*, vol. 36, pp. 89–148, Jan. 1992, doi: 10.1016/0079-6425(92)90006-S.

[23] P. Li, S. X. Li, Z. G. Wang, and Z. F. Zhang, "Fundamental factors on formation mechanism of dislocation arrangements in cyclically deformed fcc single crystals," *Prog. Mater. Sci.*, vol. 56, no. 3, pp. 328–377, Mar. 2011, doi: 10.1016/j.pmatsci.2010.12.001.

[24] S. R. Agnew and J. R. Weertman, "Cyclic softening of ultrafine grain copper," *Mater. Sci. Eng., A*, vol. 244, no. 2, pp. 145–153, Apr. 1998, doi: 10.1016/S0921-5093(97)00689-8.

[25] H. Mughrabi, "The cyclic hardening and saturation behaviour of copper single crystals," *Mater. Sci. Eng.*, vol. 33, no. 2, pp. 207–223, May 1978, doi: 10.1016/0025-5416(78)90174-X.

[26] P. Gabor, D. Canadinc, H. J. Maier, R. J. Hellmig, Z. Zuberova, and J. Estrin, "The influence of zirconium on the low-cycle fatigue response of ultrafine-grained copper," *Metallurgical Mater. Trans. A*, vol. 38, no. 9, pp. 1916–1925, Sep. 2007, doi: 10.1007/s11661-007-9230-6.

[27] J. Chen, X. Xiao, S. Xiong, J. Wang, H. Huang, and B. Yang, "Low cycle fatigue behavior of Cu-Cr-Zr alloy with different cold deformation," *Fatigue Fracture Eng. Mater. Structures*, vol. 46, no. 1, pp. 3–16, 2023, doi: 10.1111/ffe.13842.

[28] M. Liu et al., "Enhanced fatigue properties of large-scale ultrafine-grained copper fabricated by friction stir additive manufacturing and subsequent cold rolling," *Int. J. Fatigue*, vol. 183, Jun. 2024, Art. no. 108253, doi: 10.1016/j.ijfatigue.2024.108253.

[29] C. Laird, "The fatigue limits of metals," *Mater. Sci. Eng.*, vol. 22, pp. 231–236, Jan. 1976, doi: 10.1016/0025-5416(76)90159-2.

[30] R. Liu, Z. J. Zhang, and Z. F. Zhang, "The criteria for microstructure evolution of Cu and Cu-Al alloys induced by cyclic loading," *Mater. Sci. Eng., A*, vol. 666, pp. 123–138, Jun. 2016, doi: 10.1016/j.msea.2016.04.069.

[31] R. Niu, K. Han, Y.-F. Su, T. Besara, T. M. Siegrist, and X. Zuo, "Influence of grain boundary characteristics on thermal stability in nanotwinned copper," *Sci. Rep.*, vol. 6, no. 1, Aug. 2016, Art. no. 31410, doi: 10.1038/srep31410.

[32] C. E. Feltner and C. Laird, "Cyclic stress-strain response of F.C.C. metals and alloys—I phenomenological experiments," *Acta Metallurgica*, vol. 15, no. 10, pp. 1621–1632, Oct. 1967, doi: 10.1016/0001-6160(67)90137-X.

[33] R. Niu and K. Han, "Effect of notch geometry on the plastic behavior of Cu-Ag composites," *IEEE Trans. Appl. Supercond.*, vol. 34, no. 5, Aug. 2024, Art. no. 6800305, doi: 10.1109/TASC.2024.3350589.